An ultra-thin coplanar waveguide filter based on the spoof surface plasmon polaritons

Jun Wang, Lei Zhao, Zhang-Cheng Hao, and Tie Jun Cui

Citation: Appl. Phys. Lett. **113**, 071101 (2018); doi: 10.1063/1.5045069
View online: https://doi.org/10.1063/1.5045069
View Table of Contents: http://aip.scitation.org/toc/apl/113/7
Published by the American Institute of Physics

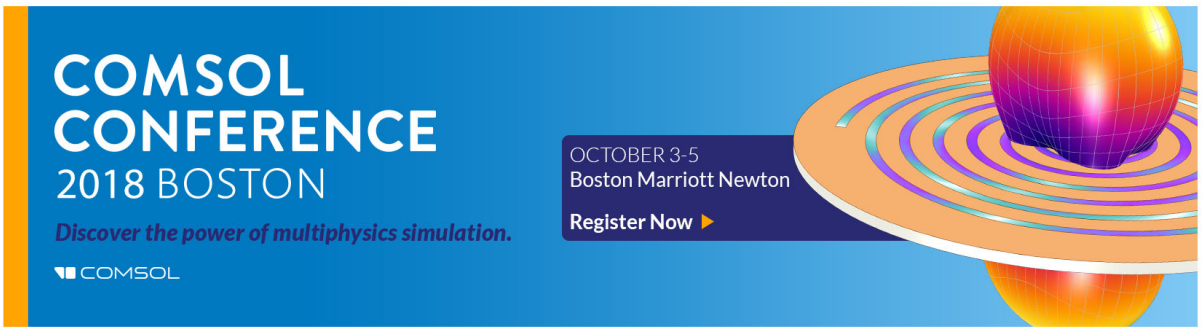

An ultra-thin coplanar waveguide filter based on the spoof surface plasmon polaritons

Jun Wang,[1,2] Lei Zhao,[2,a)] Zhang-Cheng Hao,[1] and Tie Jun Cui[1]
[1]*State Key Lab of Millimeter-Waves, School of Information Science and Engineering, Southeast University, Nanjing, Jiangsu 211189, China*
[2]*Center for Computational Science and Engineering, School of Mathematics and Statistics, Jiangsu Normal University, Xuzhou, Jiangsu 221116, China*

(Received 16 June 2018; accepted 28 July 2018; published online 14 August 2018)

In this letter, a coplanar waveguide (CPW) filter based on spoof surface plasmon polaritons (SSPPs) in the microwave frequency band is proposed, which can achieve multi-band transmission by using periodic holes etched on the middle line of a CPW. Compared to the conventional SSPP designs, the proposed SSPP-based waveguide filter removes the gradual structure for the mode conversion. Simultaneously, the transmission efficiency of high-order modes is obviously improved by employing periodic holes etched on both the side grounds of the CPW. The physical mechanism of the proposed SSPP-based waveguide filter is explained with the aid of the dispersion curves and electric field distributions. Experimental results validate the proposed concept, and the measured results are in good agreement with the simulated ones, which indicates that the proposed SSPP-based waveguide filter can find potential applications in plasmonic integrated circuits at microwave frequencies. *Published by AIP Publishing.* https://doi.org/10.1063/1.5045069

Spoof surface plasmon polaritons (SSPPs) have received a great deal of attention at microwave frequencies,[1–7] due to their ability to propagate along the textured conducting surfaces at the deep subwavelength scale. SSPPs have inherited most of the exotic performance of surface plasmon polaritons (SPPs), such as the field confinement and non-diffraction limit. Additionally, the physical performance of SSPPs can be easily controlled by optimizing the geometrical parameters.[8–14] As the advantages of the SSPPs, many different configurations based on slits, hole arrays, varactors, or blocks decorated on the metal surface are proposed for various applications.[15–32]

In order to achieve good performance, most of the SSPPs are basically excited by traditional coplanar waveguides (TCPWs),[19–22] microstrip lines (MLs),[23–25] and slot coupling (SC).[26–30] Generally, the TCPW structures were designed using gradient corrugation grooves for transmission and specific flaring grounds for mode conversion.[19–22] However, the flaring grounds are not conducive to the efficiency improvement and further miniaturization. Moreover, some two-layer ML configurations are proposed,[23–25] which have the characteristic of low loss and broadband. Meanwhile, several SSPPs using the SC excitation with an air hole at the input end of the upper slot line are proposed to enhance the SSPP performance.[26–30] However, both the ML and SC designs are two-layer structures, which are difficult to design and inflexible for integration.

In this letter, we present a kind of simple ultra-thin SSPP-based waveguide filter with periodic holes etched on the standard 50-Ω CPW, which not only has a high-efficiency low-pass transmission but also realizes a controllable multi-band performance. More importantly, the proposed structure removes the mode conversion structures used in the traditional SSPP-based waveguide filter. For better understanding of the physical mechanisms of the proposed filter, the dispersion curves and electric field distributions are carefully investigated. The characteristic of our proposed SSPP-based waveguide filter is verified through both numerical simulations and experimental measurements. The proposed design has the following features: (1) Without the gradual structures for mode conversion; (2) high low-pass transmission efficiency; (3) implementation of the controllable multi-band performance by controlling the length of the unit cell; (4) simple and flexible conformal structure can be easily integrated and miniaturized.

The configuration of the proposed SSPP-based waveguide filter is sketched in Fig. 1(a), which is a common CPW line whose middle stripline is etched with periodic holes. The proposed waveguide has two parts: one is a 50-Ω CPW feeding part and the other one is the transmission part with the periodic holes. The designed parameter of the length of the unit cell is marked as d. The unit cell of the waveguide is presented in the dashed box. The full-wave electromagnetic (EM) simulation software CST is used to calculate the design. The dispersion curves for the fundamental mode of the SSPP-based waveguide filter with different unit cell lengths (d) and hole radii (r) are presented in Fig. 1(b) and 1(c), respectively. It is obvious that the dispersion curves significantly deviate from the CPW line with the unit cell length (d) increase when r is fixed as 1.45 mm. Meanwhile, the hole radius has little influence on the dispersion curves when the unit cell length is selected as $d = 4$ mm, except that if the diameter of the hole is close to the width of the CPW line, the dispersion curves will deviate dramatically. Generally, the wave momentums of the fundamental mode gradually deviate from the CPW line and the cut-off frequency of the SSPP-based waveguide filter decreases as the unit cell length (d) and hole radius (r) increase.

a)Electronic mail: leizhao@jsnu.edu.cn

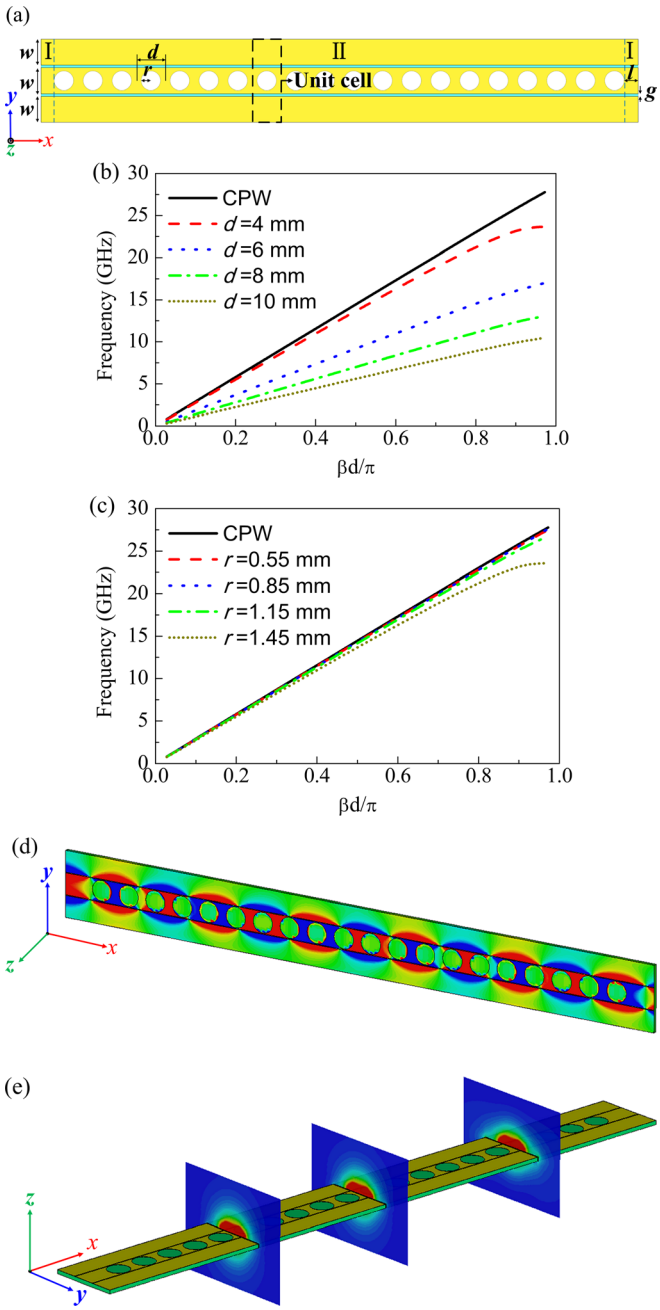

FIG. 1. (a) Configuration of the proposed SSPP-based waveguide filter, whose designed parameters are $w = 3$ mm, $l = 4$ mm, $r = 1.45$ mm, $d = 4$ mm, and $g = 0.1$ mm. Simulated dispersion curves for the fundamental mode of the proposed SSPP-based waveguide filter with (b) different unit cell lengths and (c) different hole radii. (d) The electric field distribution on the x-y plane at 15 GHz when $d = 4$ mm. (e) The magnitudes of energy flows on cross sections of the SSPP-based waveguide filter at three different locations at 15 GHz when $d = 4$ mm.

In order to further show the excellent field confinement and good propagation property of the proposed SSPP-based waveguide filter, the simulated electric field distribution on the x-y plane and the magnitudes of energy flows on cross sections at 15 GHz when $d = 4$ mm are plotted in Figs. 1(d) and 1(e). It is seen that the EM fields are highly localized on the adjacent CPW lines and adjacent holes and are tightly confined in the deep subwavelength scale around the waveguide and the SPP wave propagates, which indicate that most of the EM energy is highly localized within a small region in the proposed SSPP-based waveguide filter. Therefore, the proposed structure can support the modes of SSPP propagation on its surface, exhibiting potential applications in SSPP devices.

From the above discussions, we can find that the proposed SSPP-based waveguide filter can support the SSPP modes on the CPW surface, which means that the proposed design converts the quasi-TEM wave on the CPW to the SSPP wave efficiently by using the periodic holes etched on the CPW. Meanwhile, the periodic holes damage the boundary condition of the quasi-TEM mode which needs the transmission part to satisfy the boundary condition of the SSPP (TM) modes. As shown in Fig. 2, it is clear that the high-order TM modes appear with the increase in the unit cell length (d), and the cut-off frequency (f_{cn}) of the TM_n modes can be expressed as[33]

$$f_{cn} = \frac{k_{cn}}{2\pi\sqrt{\mu\varepsilon}}, \tag{1}$$

$$k_{cn} = k_d \frac{n}{d}, \quad n = 1, 2, 3 \cdots, \tag{2}$$

where k_{cn} is the cut-off wave number, μ and ε are the permeability and permittivity of the substrate, respectively, and k_d

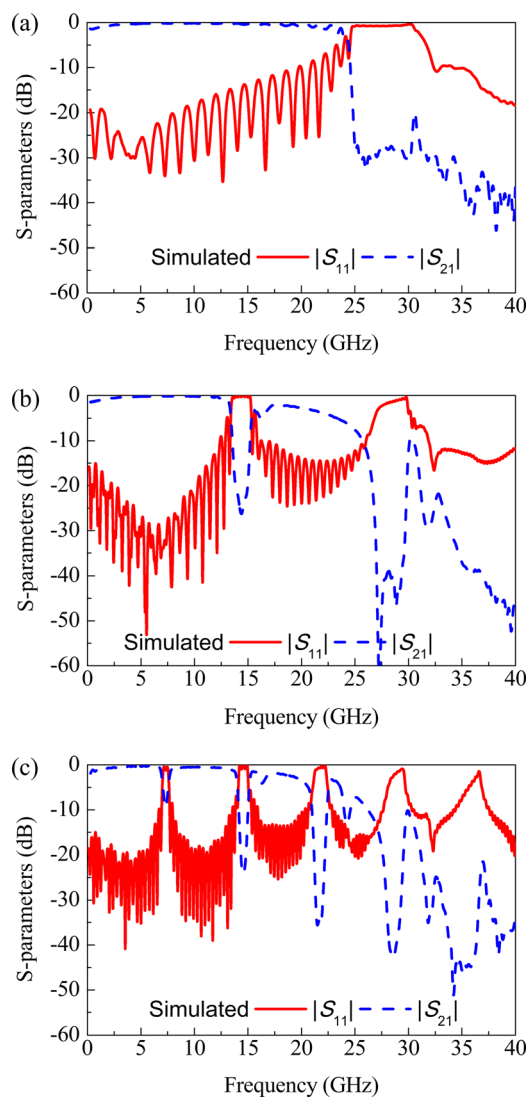

FIG. 2. S-parameters of the proposed SSPP-based waveguide filter (a) when $d = 4$ mm, (b) when $d = 8$ mm, and (c) when $d = 16$ mm.

is a constant coefficient, which can be obtained from the boundary condition and general solution of the wave equation. It should be noted that k_d will have a tiny variation with the change in d. From Eqs. (1) and (2), it is seen that the cut-off frequency of all modes is inversely proportional to the length of the unit cell (d), which means that the number of pass bands can be controlled by the distance between two adjoining holes.

In order to verify the relationship between the number of modes and unit cell lengths as formulated in Eqs. (1) and (2), the simulated cut-off frequencies of the proposed SSPP-based waveguide filter with different d values are demonstrated. In Fig. 2(a), it is clearly observed that the cut-off frequency of the fundamental mode is about 24.6 GHz when $d = 4$ mm. Moreover, as shown in Fig. 2(b), it is seen that the cut-off frequencies of the fundamental and second modes are about 13.2 GHz and 26.5 GHz, respectively, when $d = 8$ mm. Furthermore, Fig. 2(c) shows that the cut-off frequency of the fundamental, second, third, and fourth modes are about 6.9 GHz, 13.9 GHz, 21 GHz, and 28.1 GHz, respectively, when $d = 16$ mm. Additionally, it should be noted that the high-order modes will be dramatically attenuated with the frequency increase, especially above 30 GHz. From the above discussed results, we can find that the simulated cut-off frequency of high-order modes has good agreement with the proposed formulas.

Figure 2(a) shows the S-parameters of the proposed SSPP-based waveguide filter with the initial values when $d = 4$ mm. It is obvious that the SSPP-based waveguide filter achieves a single band within the designed band and its cut-off frequency of the fundamental mode is about 24.6 GHz, which agrees with the dispersion curve when $d = 4$ mm, as shown in Fig. 1(b). The simulated $|S_{21}|$ of the SSPP-based waveguide filter is high within the cut-off frequency, the highest $|S_{21}|$ is up to –0.15 dB, and the lowest $|S_{21}|$ is about −0.85 dB between 2.25 GHz and 20.7 GHz. Moreover, the simulated S-parameters of the proposed SSPP-based waveguide filter when $d = 8$ mm are shown in Fig. 2(b), which illustrates that the proposed design can achieve dual-band transmission performance with the highest $|S_{21}|$ being −0.17 dB and then the high-order modes will be attenuated gradually. Furthermore, when we increase the length of the unit cell (d) continuously, the characteristic of the multi-band will appear, as shown in Fig. 2(c). From Fig. 2, we find that the number of pass bands will be increased with the length of the unit cell (d) increased, due to the fact that cut-off frequencies of all modes will be decreased as the length of the unit cell (d) aggrandized. The pass band will disappear until the high frequency high-order modes attenuate completely. These show that the proposed SSPP-based waveguide filter with periodic holes has a good multi-band filtering characteristic. However, the transmission efficiency of the high-order modes is still flawed.

In order to overcome this blemish, a modified SSPP-based waveguide filter is proposed with the periodic hole arrays etched on the CWP striplines on the both sides, which can improve the transmission efficiency of the high-order modes efficiently, as shown in Fig. 3(a). The unit cell of the modified design is presented in the black dashed box. Moreover, it can be clearly seen from Figs. 3(b) and 3(c) that

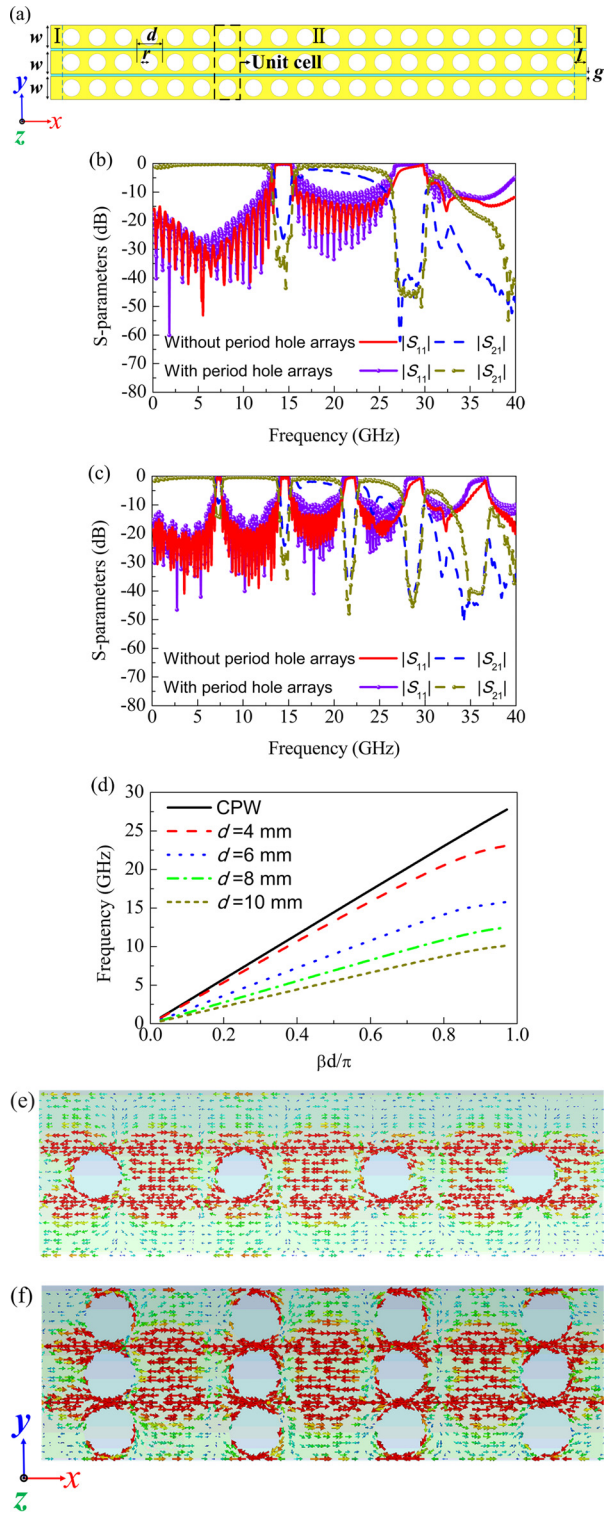

FIG. 3. (a) Configuration of the modified SSPP-based waveguide filter with periodic hole arrays. Simulated S-parameters of the proposed SSPP-based waveguide filter with and without the periodic hole arrays (b) when $d = 8$ mm and (c) when $d = 16$ mm. (d) Simulated dispersion curves for the fundamental mode of the modified SSPP-based waveguide filter with different unit cell lengths. The electric current distributions along the propagation direction at 25 GHz when $d = 8$ mm (e) with periodic hole arrays and (f) without periodic hole arrays.

the high-order mode transmission efficiency improves significantly when d increases. To gain insight into the nature of the modified SSPP-based waveguide filter mechanism, the simulated dispersion curves for the fundamental mode of the modified SSPP-based waveguide filter with different unit

cell lengths and the electric current distributions along the propagation direction at 25 GHz when $d = 8$ mm with and without periodic hole arrays are carefully investigated. From Fig. 3(d), we can find that the modified design has similar dispersion characteristics compared to the original one. Additionally, it can be clearly seen from Figs. 3(e) and 3(f) that the SPP wave is excited by the periodic hole arrays on both sides of the CPW and the S-parameter will superpose at high-order modes, leading to the high-order mode transmission efficiency improvement efficiently.

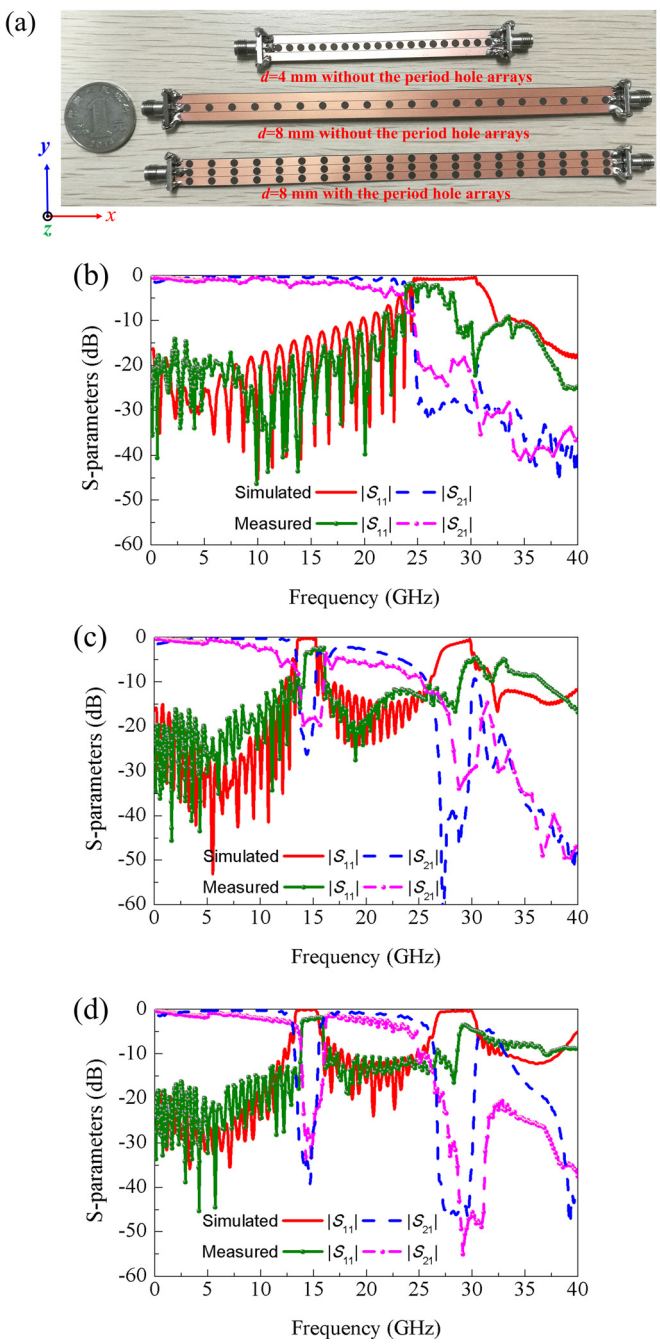

FIG. 4. (a) Photograph of the fabricated SSPP-based waveguide filter without the periodic hole arrays when $d = 4$ mm and the design with and without the periodic hole arrays when $d = 8$ mm. Measured and simulated S-parameters of the proposed SSPP-based waveguide filter (b) when $d = 4$ mm and (c) when $d = 8$ mm and (d) the modified SSPP-based waveguide filter when $d = 8$ mm.

To verify the functionality of the proposed configuration, the samples of the proposed filters with and without periodic hole arrays are fabricated, as shown in Fig. 4(a). The substrate used is 0.5 mm F4B with $\varepsilon_r = 2.65$ and loss tangent $\tan\delta = 0.0015$, and the metallic strips have a thickness of 0.018 mm. The measured results of the proposed SSPP-based waveguide filter are plotted in Figs. 4(b), 4(c), and 4(d), which show a good agreement with the simulated ones, while verifying the concept of our proposed design. Figure 4(b) shows the measured results of the proposed SSPP-based waveguide filter when $d = 4$ mm, which presents a single pass band with high transmission efficiency. Moreover, the multi-band S-parameters of the SSPP-based waveguide filter without periodic hole arrays when d increases to 8 mm are presented in Fig. 4(c), and the measured results show that the proposed design has a good multi-band characteristic. Furthermore, the measured results in Fig. 4(d) confirm that the modified SSPP-based waveguide filter can improve the transmission efficiency of the high-order modes efficiently. Additionally, it should be noted that the measured return loss of high frequencies is a little higher than the simulated ones, which may be caused by the parasitic properties of the SMA connector and substrate. As expected, the fabricated structures hold the promise to realize high performance SSPPs in microwave applications.

In conclusion, an ultra-thin SSPP-based waveguide filter is theoretically and experimentally investigated. The high low-pass transmission efficiency and multi-band characteristic are obtained by using periodic holes etched on the CPW. Specifically, the proposed waveguide need not use the gradual structure for mode conversion, which provides the ability for further miniaturization and integration. The dispersion curves and electric field distributions have been thoroughly investigated to reveal the SSPP-based waveguide filter mechanism. The prototypes of the proposed SSPP-based waveguide filter and modified design have been fabricated, and all measured results are in good agreement with the simulated ones, which validates the proposed design concept and makes it to be very useful in a variety of microwave applications.

This work was supported in part by the National Science Foundation of China under Grant Nos. 61771226, 61372057, and 61671223.

[1]J. B. Pendry, L. Martin-Moreno, and F. J. Garcia-Vidal, Science **305**, 847 (2004).
[2]F. J. Garcia-Vidal, L. Martin-Moreno, and J. B. Pendry, J. Opt. A: Pure Appl. Opt. **7**, S97 (2005).
[3]A. P. Hibbins, B. R. Evans, and J. R. Sambles, Science **308**, 670 (2005).
[4]S. A. Maier, *Plasmonics: Fundamentals and Applications* (Springer, New York, 2007).
[5]A. Kianinejad, Z. N. Chen, and C. W. Qiu, IEEE Trans. Microwave Theory Tech. **63**, 1817 (2015).
[6]A. Kianinejad, Z. N. Chen, L. Zhang, W. Liu, and C. W. Qiu, IEEE Trans. Antennas Propag. **64**, 2094 (2016).
[7]W. C. Chen, J. J. Mock, D. R. Smith, T. Akalin, and W. J. Padilla, Phys. Rev. X **1**, 021016 (2011).
[8]X. F. Zhang, L. F. Shen, and L. X. Ran, J. Appl. Phys. **105**, 013704 (2009).
[9]J. S. Liu, L. Ding, K. J. Wang, and J. Q. Yao, Opt. Express **17**, 12714 (2009).

[10]T. Jiang, L. Shen, X. Zhang, and L. Ran, Prog. Electromagn. Res. M **8**, 91 (2009).
[11]D. Martin-Cano, M. L. Nesterov, A. I. Fernandez-Dominguez, F. J. Garcia-Vidal, L. Martin-Moreno, and E. Moreno, Opt. Express **18**, 754 (2010).
[12]L. F. Shen, X. D. Chen, X. F. Zhang, and K. Agarwal, Plasmonics **6**, 301 (2011).
[13]X. Y. Liu, Y. J. Feng, B. Zhu, J. M. Zhao, and T. Jiang, Opt. Express **21**, 31155 (2013).
[14]Ory Schnitzer, Phys. Rev. B **96**, 085424 (2017).
[15]S. A. Maier, S. R. Andrews, L. Martin-Moreno, and F. J. Garcia-Vidal, Phys. Rev. Lett. **97**, 176805 (2006).
[16]Y. J. Zhou, Q. Jiang, and T. J. Cui, Appl. Phys. Lett. **99**, 111904 (2011).
[17]H. C. Zhang, W. X. Tang, J. Xu, S. Liu, J. F. Liu, and T. J. Cui, IEEE Trans. Compon. Packag. Manuf. Technol. **7**, 1486 (2017).
[18]Q. Gan, Z. Fu, Y. J. Ding, and F. J. Bartoli, Phys. Rev. Lett. **100**, 256803 (2008).
[19]L. L. Liu, Z. Li, C. Q. Gu, P. P. Ning, B. Z. Xu, Z. Y. Niu, and Y. J. Zhao, J. Appl. Phys. **116**, 013501 (2014).
[20]H. F. Ma, X. P. Shen, Q. Cheng, W. X. Jiang, and T. J. Cui, Laser Photonics Rev. **8**, 146 (2014).
[21]B. C. Pan, Z. Liao, J. Zhao, and T. J. Cui, Opt. Express **22**, 13940 (2014).
[22]L. Zhao, X. Zhang, J. Wang, W. H. Yu, J. D. Li, H. Su, and X. P. Shen, Sci. Rep. **6**, 36069 (2016).
[23]Z. Liao, J. Zhao, B. C. Pan, X. P. Shen, and T. J. Cui, J. Phys. D: Appl. Phys. **47**, 315103 (2014).
[24]H. C. Zhang, S. Liu, X. P. Shen, L. H. Chen, L. M. Li, and T. J. Cui, Laser Photonics Rev. **9**, 83 (2015).
[25]W. J. Zhang, G. Q. Zhu, L. G. Sun, and F. J. Lin, Appl. Phys. Lett. **106**, 021104 (2015).
[26]X. Gao, L. Zhou, Z. Liao, H. F. Ma, and T. J. Cui, Appl. Phys. Lett. **104**, 191603 (2014).
[27]Q. X. Xiao, B. J. Yang, and Y. J. Zhou, J. Appl. Phys. **118**, 233112 (2015).
[28]Y. J. Zhou and Q. X. Xiao, J. Appl. Phys. **121**, 123109 (2017).
[29]Y. J. Guo, K. D. Xu, and X. H. Tang, Opt. Express **26**, 10589 (2018).
[30]Y. J. Guo, K. D. Xu, Y. H. Liu, and X. H. Tang, IEEE Access **6**, 10249 (2018).
[31]H. C. Zhang, P. H. He, X. X. Gao, W. X. Tang, and T. J. Cui, J. Phys.: Condens. Matter **30**, 134004 (2018).
[32]D. W. Zhang, K. Zhang, Q. Wu, R. W. Dai, and X. J. Sha, Opt. Lett. **43**, 003176 (2018).
[33]D. M. Pozar, *Microwave Engineering*, 3rd ed. (Wiley, New York, 2005).